ANTIOXIDANTS & REDOX SIGNALING
Volume 16, Number 1, 2012

DOI: 10.1089/ars.2010.3844

ORIGINAL RESEARCH COMMUNICATION

Disruption of Caveolae Blocks Ischemic Preconditioning-Mediated S-Nitrosylation of Mitochondrial Proteins

Junhui Sun,[1] Mark J. Kohr,[1,2] Tiffany Nguyen,[1] Angel M. Aponte,[1,3] Patricia S. Connelly,[4] Shervin G. Esfahani,[4] Marjan Gucek,[1,3] Mathew P. Daniels,[4] Charles Steenbergen,[2] and Elizabeth Murphy[1]

Abstract

Aims: Nitric oxide (NO) and protein S-nitrosylation (SNO) play important roles in ischemic preconditioning (IPC)-induced cardioprotection. Mitochondria are key regulators of preconditioning, and most proteins showing an increase in SNO with IPC are mitochondrial. The aim of this study was to address how IPC transduces NO/SNO signaling to mitochondria in the heart. ***Results:*** In this study using Langendorff perfused mouse hearts, we found that IPC-induced cardioprotection was blocked by treatment with either *N*-nitro-L-arginine methyl ester (L-NAME, a constitutive NO synthase inhibitor), ascorbic acid (a reducing agent to decompose SNO), or methyl-β-cyclodextrin (MβCD, a cholesterol sequestering agent to disrupt caveolae). IPC not only activated AKT/eNOS signaling but also led to translocation of eNOS to mitochondria. MβCD treatment disrupted caveolar structure, leading to dissociation of eNOS from caveolin-3 and blockade of IPC-induced activation of the AKT/eNOS signaling pathway. A significant increase in mitochondrial SNO was found in IPC hearts compared to perfusion control, and the disruption of caveolae by MβCD treatment not only abolished IPC-induced cardioprotection, but also blocked the IPC-induced increase in SNO. ***Innovation:*** These results provide mechanistic insight into how caveolae/eNOS/NO/SNO signaling mediates cardioprotection induced by IPC. ***Conclusion:*** Altogether these results suggest that caveolae transduce eNOS/NO/SNO cardioprotective signaling in the heart. *Antioxid. Redox Signal.* 16, 45–56.

Introduction

Ischemic preconditioning (IPC) is an adaptive phenomenon whereby brief episodes of myocardial ischemia and reperfusion render the heart resistant to subsequent prolonged ischemic injury (23). IPC initiates a number of signaling pathways at the plasma membrane, which are transduced to the mitochondria (9, 22). Among them, nitric oxide (NO) is important in IPC-induced cardioprotection (3, 14). In addition to activating cyclic guanosine monophosphate (cGMP)/protein kinase G (PKG)-dependent signaling pathways, NO can directly modify protein sulfhydryl residues through protein S-nitrosylation (SNO), which has emerged as an important post-translational protein modification in cardiovascular signaling (17, 29) and cardioprotection (18, 34). In recent studies, we have reported that IPC results in increased SNO of a number of proteins involved in cardioprotection, and most of these SNO proteins are mitochondrial proteins (15, 33).

It has been reported that blocking the internalization of signaling molecules associated with G-protein-coupled receptors inhibits cardioprotection afforded by IPC (37). Consistent with this concept, Quinlan *et al.* have found that preconditioning induces the assembly of a caveolar signaling platform that migrates to mitochondria to induce mitochondrial ATP-dependent potassium channel opening (27). Caveolae are flask-like invaginations of the plasma membrane

Innovation

Myocardial caveolae have recently been implicated in cardioprotection, but the underlying mechanistic basis has not been explored in detail. In this study, the authors provide novel data showing that caveolae transduce eNOS/NO/SNO signaling to the mitochondria, and that disruption of caveolae by MβCD treatment blocks this important cardioprotective signaling pathway. These results not only suggest that caveolae signaling complexes are crucial for IPC, but also point out a possible caveolae-mediated eNOS/NO/SNO cardioprotective signaling network between caveolae and mitochondria.

[1]Systems Biology Center, [3]Proteomics Core Facility, and [4]Electron Microscopy Core Facility, National Heart Lung and Blood Institute, National Institutes of Health, Bethesda, Maryland.
[2]Department of Pathology, Johns Hopkins Medical Institutions, Baltimore, Maryland.

enriched with cholesterol, sphingolipids, and the marker protein, caveolin. Caveolae are also enriched in other signaling molecules and thus play an important role in signaling (24, 26). The caveolin gene family consists of three isoforms: caveolin-1, -2, and -3. The first two caveolin isoforms are co-expressed in a variety of cell types, while caveolin-3 is a muscle-specific isoform (32, 36). In cardiomyocytes, caveolin-3 acts as a scaffolding protein to concentrate and organize molecules (11, 26) such as endothelial NO synthase (eNOS) within the caveolae to mediate signal transduction (5, 6). Recent studies suggested that caveolae and caveolin-3-associated signaling play an important role in preconditioning-mediated cardioprotection (4, 10, 16, 38). For example, the gene knockout of caveolin-3 abolished IPC-induced protection (10), while the cardiac-specific overexpression of caveolin-3 led to protection that mimicked IPC (38).

The goal of this study was to examine whether caveolae play an important role in regulating compartmentalized eNOS/NO/SNO signaling in IPC-induced cardioprotection. In the present study, methyl-β-cyclodextrin (MβCD), a cholesterol sequestering reagent, was infused into Langendorff perfused mouse hearts to disrupt caveolar structure in cardiomyocytes (4, 25). Two dimensional DyLight fluorescence difference gel electrophoresis (2D DyLight DIGE) (19, 33) was employed to determine whether there are differences in protein S-nitrosylation. Consistent with the hypothesis, we found that disruption of caveolae abolished the protection afforded by IPC and blocked IPC-mediated SNO signaling.

Results

We showed previously that IPC leads to an increase in SNO of mitochondrial proteins (15, 33). Others have reported that loss of caveolin-3 (caveolin-3$^{-/-}$) blocks protection afforded by IPC (38). Thus the aim of this study was to test the hypothesis that caveolae-dependent signaling is required for the IPC-mediated increase in SNO of mitochondrial proteins. If caveolae are required for IPC-mediated SNO of mitochondrial proteins, then disruption of caveolae with MβCD, a cholesterol sequestering agent, should block the protection provided by IPC and should also block the increase of SNO that occurs with IPC.

MβCD treatment disrupted caveolae and attenuated eNOS signaling in the caveolae

To first confirm that MβCD results in disruption of caveolae without a general disruption of cell structure, we used transmission electron microscopy to examine cell morphology. Transmission electron microscopy (Fig. 1A) clearly demonstrated that MβCD treatment (1 mmol/L for 30 min perfusion) disrupted caveolae. MβCD treatment decreased the number of caveolae per μm sarcolemma from 0.31 ± 0.03 for perfusion control ($n = 4$) to 0.11 ± 0.01 for MβCD-treated hearts ($n = 3$, $p < 0.01$). However, MβCD treatment did not change mitochondrial morphology or the myofibrillar structure. To further confirm that MβDC lead to disruption of caveolae, we used a detergent-free Na_2CO_3 (pH 11) method (32) to isolate caveolae-enriched fractions. As shown in Figure 1B, the disruption of caveolae by MβCD treatment led to the disappearance of the single light-scattering buoyant caveolae-enriched fraction (fraction 5) and caused migration of caveolin-3 and other associated proteins into heavier fractions of the sucrose gradients (fractions 8–12).

Numerous studies have demonstrated that eNOS is localized in caveolae via interaction with caveolin, and this compartmentalization facilitates dynamic protein–protein interactions and signal transduction events that modify eNOS activity (5, 21, 30). Caveolin-3 has been shown to be the muscle-specific caveolin. However, our whole heart homogenate contains both myocyte and endothelial cells. To evaluate the relative proportion of eNOS bound to caveolin-1 versus caveolin-3, we performed an IP of eNOS using anti-caveolin-1/caveolin-3 *vs.* either anti-caveolin-1 or anti-caveolin-3 alone in total heart homogenate (Fig. 2A). IP with anti-caveolin-1/caveolin-3 will pull down both the endothelial and myocardial eNOS, whereas IP with anti-caveolin-3 should only pull down myocardial eNOS. If caveolin-1 binds both myocardial eNOS and endothelial eNOS, then anti-caveolin-1 IP should pull down higher levels of eNOS than that by anti-caveolin-3 IP, which was not observed (see Fig. 2A). The data in Figure 2A suggest a specific interaction of myocardium-derived eNOS with caveolin-3, the muscle-specific isoform of caveolin. We next wanted to determine if MβCD treatment alters the interaction of eNOS with caveolin-3 in cardiomyocytes. As shown in Figure 2B, disruption of caveolae by MβCD treatment significantly decreased the association of eNOS with caveolin-3, thus significantly attenuating the compartmentalization of eNOS signaling in the caveolae.

Disruption of caveolae by MβCD treatment abolished IPC-induced cardioprotection

Perfusion of hearts with MβCD alone did not change cardiac hemodynamics (Table 1). In addition, MβCD treatment alone did not lead to changes of post-ischemic functional recovery (Table 1, Fig. 3B) or infarct size (Fig. 3C). However, MβCD treatment prior to and during IPC abolished IPC-induced cardioprotection (Table 1, Fig. 3). Thus, consistent with previous data in the literature (4), treatment of Langendorff perfused heart with MβCD to disrupt caveolae blocked IPC-induced cardioprotection. These data suggest that caveolae play an important role in mediating the cardioprotective effects of IPC (4, 10, 16, 38).

MβCD treatment prevented IPC-induced increase in protein S-nitrosylation

To test if caveolae are necessary for eNOS/NO/SNO signaling in IPC, we examined whether disruption of caveolae with MβCD blocks SNO signaling. Total heart homogenate fractions were subjected to 2D DyLight DIGE proteomic analysis to detect SNO in IPC $\pm$ MβCD hearts. A representative 2D DyLight DIGE gel is shown in Figure 4. SNO proteins in perfusion control hearts were labeled by DyLight 488 (green), IPC hearts were labeled with DyLight 649 (red), and MβCD-treated IPC hearts were labeled with DyLight 549 (yellow). As shown in Figure 4 and Table 2, IPC significantly increased SNO signaling. MβCD treatment blocked the increase in SNO induced by IPC (overlay of DyLight 549/649), and the SNO level in MβCD-treated hearts was comparable to that in the perfusion control (overlay of DyLight 488/549). The fluorescent spots indicate SNO proteins, which were extracted and identified by mass spectrometry. Data from multiple gels ($n = 3$) were compiled in Table 2, which shows that IPC (without MβCD) leads to an increase in SNO of

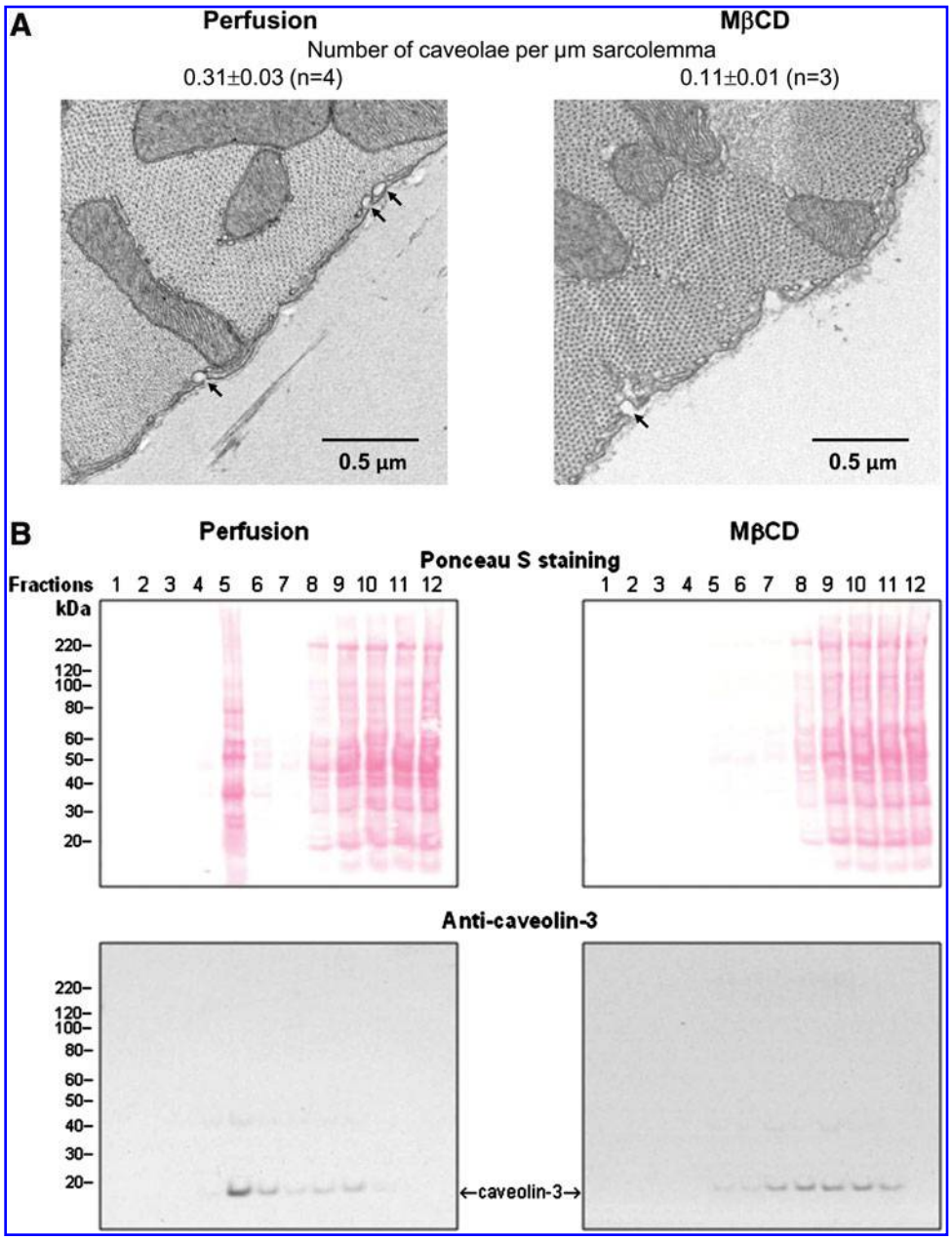

FIG. 1. MβCD treatment disrupted caveolae structure at the sarcolemma. (A) Transmission electron microscope cross-sectional images of left ventricle show that caveolae were localized at the sarcolemmal membrane (*arrows*), and M*β*CD treatment decreased the number of caveolae in the sarcolemma but did not change mitochondrial morphology or the myofibril array. **(B)** Sucrose gradient centrifugation was used to isolate caveolae-enriched fractions as described in Materials and Methods. Equal volumes from each fraction collected from the top to the bottom was separated by 4%–12% SDS-PAGE and transferred to nitrocellulose membranes. After Ponceau S staining (*top panels*), the membranes were subjected to anti-caveolin-3 immunoblot analysis (*bottom panels*). M*β*CD treatment disrupted caveolar structure and composition, as seen in the disappearance of the caveolin-3-enriched fraction (fraction 5). The data shown is representative of six individual preparations for each group. (To see this illustration in color the reader is referred to the web version of this article at www.liebertonline.com/ars).

proteins. The ratio of ~1:1 of (M*β*CD+IPC)/Perf (Table 2) in DyLight intensity (SNO content) of each protein spot suggests that the disruption of caveolae in hearts by M*β*CD treatment prevented IPC-induced activation of SNO signaling. These data are consistent with the hypothesis that disruption of caveolae disrupts eNOS/NO/SNO signaling.

To confirm a role for SNO in IPC, the effects of constitutive NOS inhibition with *N*-nitro-L-arginine methyl ester (L-NAME) or decomposing SNO with ascorbic acid were tested in the Langendorff perfused mouse heart IPC-I/R model (Fig. 5A). L-NAME (10 *μ*mol/L) treatment alone did not change pre-ischemic hemodynamics, post-ischemic recovery of LVDP, or infarct size in nonpreconditioned hearts. However, treatment with L-NAME 10 min prior to and during IPC blocked IPC-induced cardioprotection (Fig. 5B). Ascorbic acid (1 mmol/L) treatment did not change the pre-ischemic heart rate, but caused an ~50% decrease in pre-ischemic LVDP. We were concerned that this pre-ischemic decrease in LVDP might alter the response to ischemia; however we found that addition of ascorbic acid did not alter infarct size or recovery of function following ischemia-reperfusion in hearts in non-IPC hearts. This would suggest that the pre-ischemic decrease in LVDP is not altering infarct size. However, 5 min of ascorbic acid treatment in the last cycle of IPC prior to ischemia abolished IPC-induced cardioprotection (Fig. 5C). These results suggested that NO/SNO signaling plays an essential role in IPC-induced acute cardioprotection.

MβCD treatment blocked IPC-induced activation of the AKT/eNOS signaling pathway

We were also interested in determining if disruption of caveolae altered cardioprotective signaling that leads to activation of eNOS. Studies have shown that AKT can directly

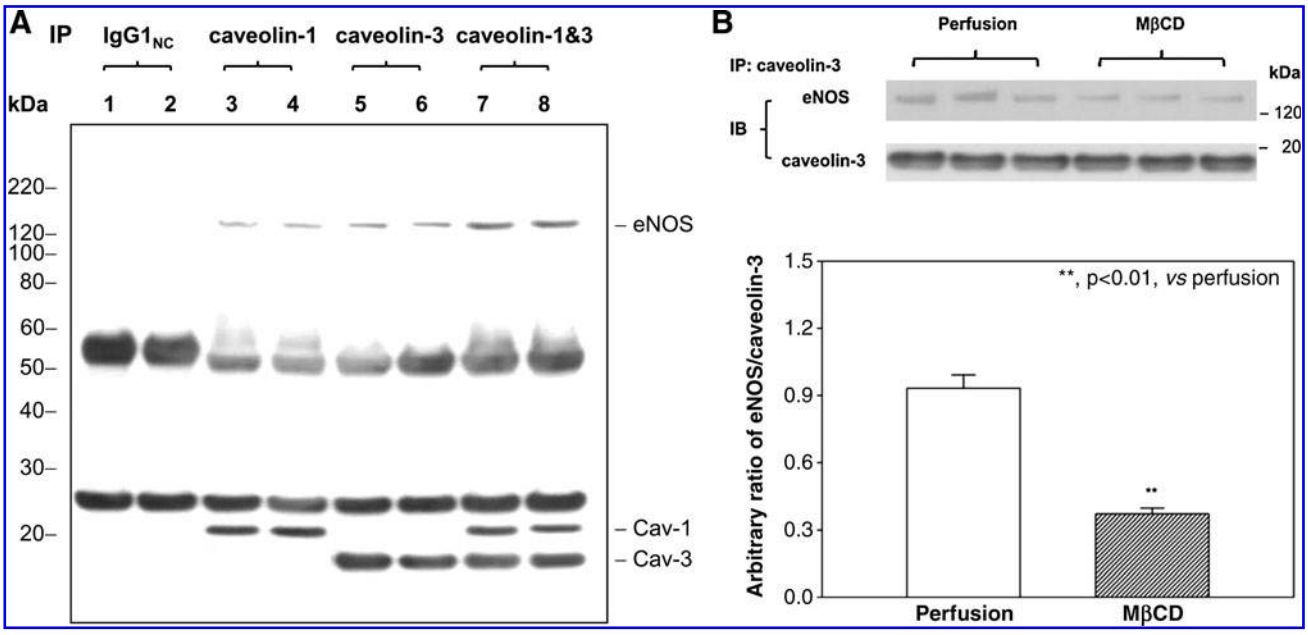

FIG. 2. MβCD treatment decreased the association of eNOS with caveolin-3. (A) A representative immunoblot of anti-caveolin immunoprecipitation (IP) from two perfusion control hearts. As described in Materials and Methods, samples of total heart homogenate were immunoprecipitated with negative control nonimmune IgG1 ($IgG1_{NC}$), anti-caveolin-1 antibody, anti-caveolin-3 antibody, or both anti-caveolin-1 and -3 antibodies. Two bands at ~55 kDa and ~25 kDa were nonspecific IgG heavy and light chain, respectively. **(B)** A representative immunoblot of anti-caveolin-3 IP from three individual hearts with and without MβCD treatment for each group and densitometric analysis for the arbitrary ratio of eNOS *vs.* caveolin-3. $^{**}p < 0.01$, *vs.* perfusion control ($n = 5$ in each group).

phosphorylate and activate eNOS, leading to activation of NO signaling (31, 39). Immunblot analysis using total heart homogenates (Fig. 6) showed that IPC significantly increased phosphorylation of AKT (p-AKT) at Ser 473 and phosphorylation of eNOS (p-eNOS) at Ser1177 (equivalent to Ser1176 in mouse), while treatment with MβCD blocked phosphorylation of AKT and eNOS in IPC hearts. Thus, IPC-induced AKT-eNOS cardioprotective signaling pathways are blocked by MβCD treatment.

Caveolae transduced eNOS/NO/SNO signaling in IPC hearts

We have demonstrated that disruption of caveolae by MβCD treatment not only abolished IPC-induced cardioprotection (Fig. 3), but also blocked eNOS signaling (Figs. 2 and 6) and prevented the increase in SNO induced by IPC (Fig. 4). As noted, IPC leads to an increase in SNO of a large number of mitochondrial proteins (Table 2) (15, 33). These data are consistent with the hypothesis, which has also been suggested by other recent studies (12, 20, 28), that caveolae-mediated endocytosis plays a role in regulating eNOS and delivering NO to subcellular targets (*e.g.*, mitochondria). To further test this hypothesis, we prepared mitochondria fractions from Langendorff-perfused mouse hearts immediately after perfusion and IPC. Equal amounts of mitochondrial proteins from each heart sample were separated by 4%–12% SDS-PAGE and transferred to nitrocellulose membranes. The Ponceau S staining confirms similar protein loading (Fig. 7A). VDAC-1 was used as a mitochondrial and equal-loading marker (Fig. 7B). We saw no detectable caveolin-1 (~20 kDa) in the mitochondria prepared from either perfusion control or IPC hearts. Although the mitochondria isolated from perfusion control hearts did not contain caveolin-3 (~18 KDa), caveolin-3 was detected in mitochondrial samples isolated from IPC hearts. In addition, IPC significantly increased levels of eNOS in mitochondria, in parallel to the change in caveolin-3. These data support the hypothesis that IPC results in mobilization of caveolae, which transduces eNOS/NO/SNO signaling to the end effector mitochondria, leading to cardioprotection.

Discussion

Both eNOS and neuronal NOS (nNOS) are constitutively expressed in cardiomyocytes but within distinct subcellular locations, *i.e.*, eNOS is predominantly localized at caveolae in the sarcolemma (1, 7) and nNOS is mostly localized to the sarcoplasmic reticulum (1, 41). In this study, we found that perfusion with a constitutive NOS inhibitor L-NAME prior to and during IPC abolished IPC-induced protection (Fig. 5), suggesting that the activation of constitutive NOS is necessary for IPC-induced acute cardioprotection. Consistent with this finding, loss of IPC-induced cardioprotection has been found in $eNOS^{-/-}$ mouse hearts (35), although there are data to the contrary (8).

There are emerging data suggesting that protein S-nitrosylation plays an important role in cardioprotection (17, 18, 33, 34). Our studies have demonstrated that IPC results in an increase in SNO, and that SNO can alter protein activity and protect proteins against further oxidation (15, 33, 34). A previous study by our group reported that IPC was blocked by N-acetylcysteine, a glutathione precursor and reducing agent, suggesting a redox-sensitive mechanism is involved in

TABLE 1. HEMODYNAMIC PARAMETERS

Heart samples	(n)	BW (g)	Pre-MβCD equilibration				Post-MβCD prior to IPC				End of reperfusion			
			FR (ml/min)	HR (bpm)	LVDP (cmH_2O)	$+dp/dt$ $-dp/dt$ (cmH_2O/ms)	FR (ml/min)	HR (bpm)	LVDP (cmH_2O)	$+dp/dt$ $-dp/dt$ (cmH_2O/ms)	FR (ml/min)	HR (bpm)	LVDP (cmH_2O)	$+dp/dt$ $-dp/dt$ (cmH_2O/ms)
Perf-I/R	5	26.7±0.4	2.4±0.2	361±13	137±8	6.8±0.5 −4.4±0.2					1.8±0.1	339±12	55±9	3.6±0.2 −3.5±0.2
MβCD-I/R	6	27.1±0.5	2.5±0.3	365±14	139±9	6.7±0.4 −4.3±0.4	2.3±0.4	357±15	132±8	6.3±0.4 −4.3±0.4	1.8±0.3	341±13	43±6	3.4±0.3 −3.3±0.3
Perf-IPC-I/R	5	26.9±0.3	2.4±0.2	359±16	128±8	6.5±0.4 −4.2±0.3					1.9±0.2	338±15	92±10**	3.9±0.3 −3.6±0.3
MβCD-IPC-I/R	6	26.4±0.4	2.3±0.2	351±10	133±6	6.3±0.5 −4.1±0.3	2.1±0.2	331±18	128±9	6.2±0.4 −3.8±0.3	1.7±0.2	321±17	26±6**	2.6±0.3** −2.1±0.2**

Values are mean±SE; *n*, number of hearts; BW, body weight; FR, flow rate; HR, heart rate (beats per min, bpm); LVDP, left ventricular developed pressure; ± dp/dt, rates of pressure rise and fall, respectively. **$p < 0.01$, *vs.* other groups.

the protection afforded by IPC (2). In this study, the inhibition of IPC-induced cardioprotection by ascorbic acid (Fig. 5), a reducing agent that specifically decomposes SNO, provides strong evidence showing that SNO signaling plays an important role in IPC-induced cardioprotection. Consistent with our recent studies (15, 33), the majority of proteins with an increase in SNO after IPC were mitochondrial proteins (Fig. 4 and Table 2).

In this study, we tested the hypothesis that caveolae-associated eNOS/NO is important for SNO of mitochondrial proteins in IPC hearts. In support of the hypothesis, data in the literature show that that IPC increased the formation of caveolae, and a transgenic mouse with cardiomyocyte-specific overexpression of caveolin-3 showed enhanced formation of caveolae and exhibited reduced ischemia/reperfusion (I/R) injury (38). In addition, caveolin-$3^{-/-}$ mice showed no protection in response to IPC (38). A recent study by Quinlan *et al.* (27) has shown that preconditioning the heart induces formation of signalosomes, caveolae-associated signaling platforms that interact with mitochondria to open mitochondrial ATP-dependent potassium channels (27). These data not only suggest that caveolae signaling complexes are crucial for IPC, but also point out a possible cardioprotective signaling network between caveolae and mitochondria. It has been suggested that activated eNOS could be internalized to deliver NO to subcellular targets for biological effects (12, 20, 28). In this study, we found that M*β*CD treatment not only abolished IPC-induced cardioprotection (Fig. 3), but also markedly reduced the association of eNOS with caveolin-3 (Fig. 2) and IPC-induced phosphorylation of eNOS (Fig. 6). Furthermore, M*β*CD treatment blocked the IPC-induced increase in SNO (Fig. 4, Table 2). The parallel changes in caveolar eNOS signaling and SNO in mitochondria in IPC hearts are consistent with the hypothesis that activation of eNOS and caveolae trafficking to mitochondria are important in generating mitochondrial-localized eNOS/NO/SNO signaling. The detection of eNOS/caveolin-3 in mitochondria isolated from IPC hearts (Fig. 7) provides support for this hypothesis.

As caveolae are important for many signaling pathways, the disruption of caveolae could inhibit protection by blocking any number of signaling pathways. Thus, one limitation of this study is that we only examined the role of caveolin-3/eNOS/SNO, but did not investigate other signaling pathways such as the NO/guanylyl cyclase/cGMP/PKG pathway. However, it is clear that eNOS/NO/SNO signaling is one of the signaling pathways that is blocked by disruption of caveolae. Since SNO had been previously shown to play a role in cardioprotection, it is likely that disruption of this signaling pathway contributes to loss of cardioprotection. Because of dynamic range issues, most of the proteomic methods (2D gels and mass spectrometry) are biased toward detection of high-abundance proteins (34). Thus, the prevalence of mitochondrial proteins identified as SNO proteins might be due in part to their high abundance. Our recent study using a SNO-RAC proteomic approach confirms that most of SNO proteins in IPC hearts are mitochondrial proteins (15), suggesting that mitochondria are indeed one of the major subcellular organelles targeted by SNO signaling in IPC hearts.

In summary, we found that M*β*CD treatment not only disrupted caveolae and association of eNOS with caveolin-3, but

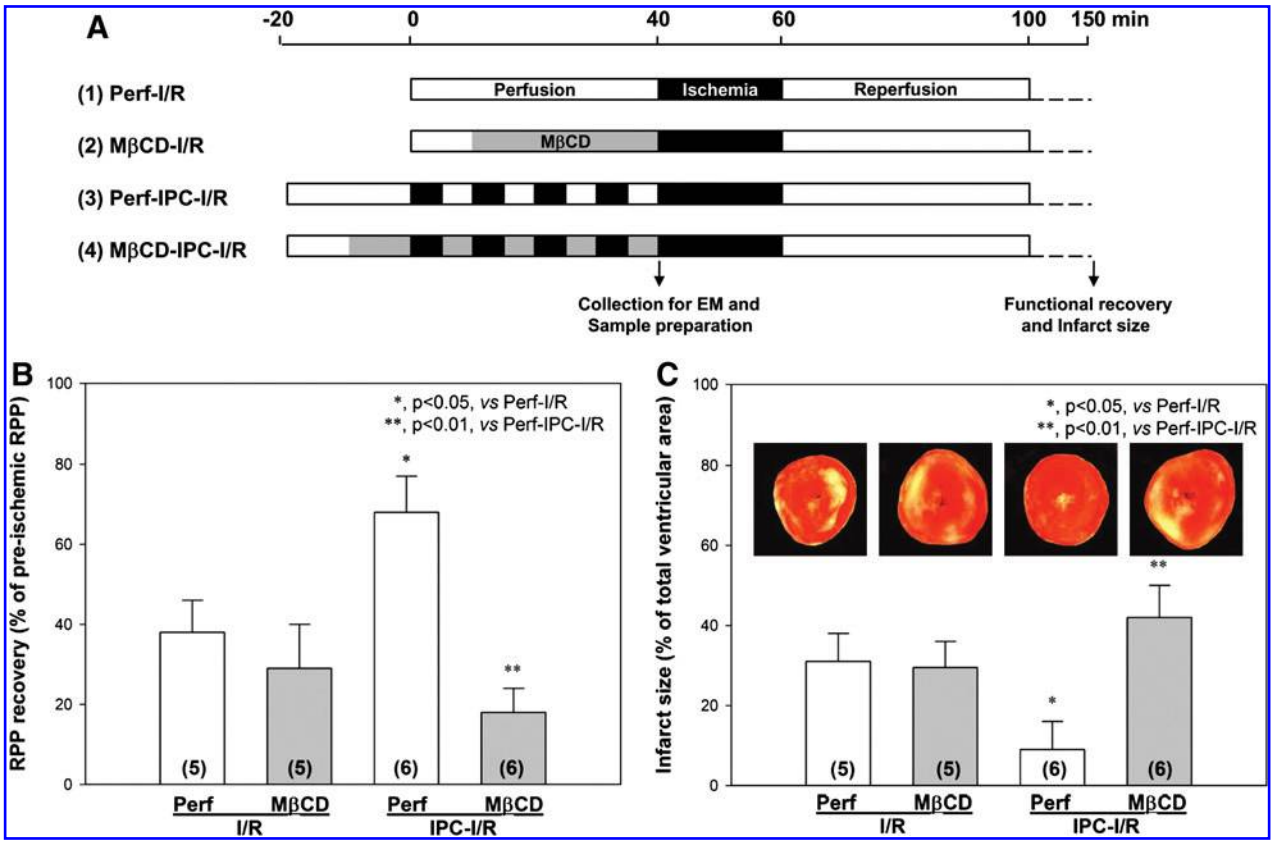

FIG. 3. MβCD treatment abolished IPC-induced cardioprotection. (A) IPC-I/R protocol with MβCD (1 mmol/L) administration; **(B)** Post-ischemic left ventricular RPP functional recovery; **(C)** Infarct size, measured at the end of reperfusion by 1% TTC staining. Inset, representative infarct images from each group. $*p < 0.05$ *vs.* Perf-I/R, and $**p < 0.01$ *vs.* Perf-IPC-I/R. *n*, number of animals in each group. (To see this illustration in color the reader is referred to the web version of this article at www.liebertonline.com/ars).

also blocked IPC-induced cardioprotection and the increase in SNO of mitochondrial proteins that normally occur with cardioprotection. These data are consistent with the hypothesis that caveolin-3-associated eNOS/NO trafficking between plasma membrane and mitochondria provide an important signaling pathway regulating SNO of mitochondrial proteins.

Materials and Methods

Animals

C57BL/6J male mice were obtained from Jackson Laboratories (Bar Harbor, Maine) and were between 12 and 16 weeks old at the time of experimentation. All animals were treated in accordance with National Institutes of Health guidelines and the "Guiding Principles for Research Involving Animals and Human Beings." This study was reviewed and approved by the Institutional Animal Care and Use Committee of the National Heart Lung and Blood Institute.

Langendorff heart perfusion and IPC-ischemia/reperfusion protocol

Mice were anesthetized with pentobarbital and anticoagulated with heparin. Hearts were excised quickly and placed in ice-cold Krebs-Henseleit buffer (in mmol/L: 120 NaCl, 11 D-glucose, 25 $NaHCO_3$, 1.75 $CaCl_2$, 4.7 KCl, 1.2 $MgSO_4$, and 1.2 KH_2PO_4). The aorta was cannulated on a Langendorff apparatus and the heart was perfused in retrograde fashion with Krebs-Henseleit buffer at a constant pressure of 100 cm of water at 37°C. Krebs-Henseleit buffer was oxygenated with 95% O_2/5% CO_2, and maintained at pH 7.4. After equilibrium perfusion or IPC (4 cycles of 5 min of ischemia and 5 min of reperfusion), mouse hearts were subjected to 20 min of no-flow ischemia, followed by 90 min of reperfusion. Drug administration is illustrated for each IPC-I/R protocol in corresponding figures. To prevent SNO breakdown, Langendorff perfusion and sample preparations were carried out in the dark.

Hemodynamic and infarct size measurements

To monitor left ventricular contractile function, a latex balloon connected to a pressure transducer was inserted into the left ventricle of a Langendorff perfused heart. The left ventricular developed pressure (LVDP) was recorded and digitized using a PowerLab system (ADInstruments, Colorado Springs, CO). We used the rate pressure product (RPP = LVDP × heart rate) as a measure of function. The post-ischemic functional recovery was expressed as percentage of preischemic RPP during the equilibrium period. For measurement of myocardial infarct size, hearts were perfused with 1% (w/v) of 2,3,5-triphenyltetrazolium chloride (TTC) after 90 min of reperfusion and incubated in TTC at 37°C for 15 min, followed by fixation in 10% (w/v) formaldehyde. Infarct size was expressed as the percentage of total area of cross-sectional slices through the ventricles.

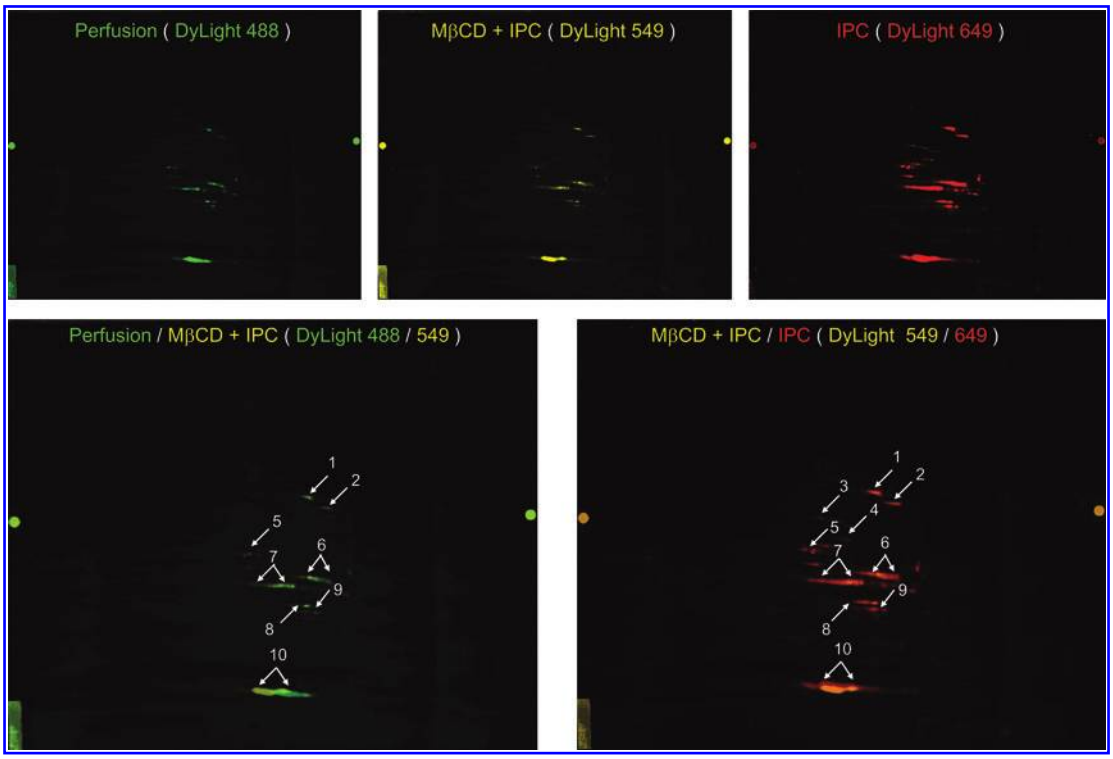

FIG. 4. Differences in protein S-nitrosylation in total heart homogenate isolated from perfusion control and IPC hearts with and without MβCD treatment. *Top panels*: a representative 2D DyLight DIGE gel was scanned at each of the distinct wavelengths of the DyLight fluors, showing a pattern of protein SNO for that particular treatment group. *Bottom left panel*: overlaid images of DyLight 488 (perfusion control, *green*) *vs.* 549 (MβCD + IPC, *yellow*). *Bottom right panel*: overlaid images of DyLight 549 (MβCD + IPC, *yellow*) *vs.* DyLight 649 (IPC, *red*). The protein spots were picked for MS/MS analysis, and are listed in Table 2.

Total heart homogenate preparation

Total heart homogenate was obtained by grinding a snap-frozen mouse heart into powder in liquid nitrogen, followed by homogenization with a tight-fitting glass Dounce homogenizer on ice in 1.5 ml homogenate buffer containing (in mmol/L, pH7.4): 70 NaCl, 20 HEPES, 2.5 $MgCl_2$, 1 EDTA, 0.1 neocuproine (a copper chelating agent), and 0.5% (v/v) Triton X-100 with protein protease/phosphatase inhibitors (Roche Diagnostics, Indianapolis, IN). The mixture was kept on ice for 60 min with gentle vortex mixing every 15 min. The sample was homogenized again on ice using a Dounce glass

Table 2. MβCD Treatment Abolished IPC-Induced Increase of Protein S-Nitrosylation in Total Homogenate of Mouse Heart

Spots number	*Accession number*	*Protein name*	*Protein Mw*	*Protein pI*	*Peptide count*	*MS/MS C.I.%*	*SNO level (Arbitrary ratio of DyLight intensity)* IPC/Perf	MβCD+IPC/Perf	IPC/MβCD+IPC
1	Q99KI0	Aconitate hydratase, mitochondrial	85464	8.08	29	100	6.1 ± 0.7*	1.2 ± 0.2	5.1 ± 0.6*
2	Q8BMS1	Mitochondrial trifunctional enzyme subunit α	82670	9.24	37	100	5.3 ± 0.6*	1.4 ± 0.1	3.8 ± 0.4*
3	Q91VD9	Mitochondrial complex I-75 KDa	79749	5.51	22	100	–	–	–
4	Q921G7	Electron transfer flavoprotein dehydrogenase	68091	7.34	17	100	–	–	–
5	Q03265	Mitochondrial F1F0 ATPase subunit α	59753	9.22	24	100	4.0 ± 0.4*	1.1 ± 0.3	3.6 ± 0.4*
6	Q6P8J7	Creatine kinase, sarcomeric	47899	8.64	20	100	4.9 ± 0.6*	1.2 ± 0.2	4.1 ± 0.5*
7	P07310	Creatine kinase, M-type	43045	6.58	7	96.4	5.1 ± 0.8*	1.6 ± 0.5	3.2 ± 0.6*
8	P14152	Malate dehydrogenase, cytoplasmic	36511	6.16	8	99.3	2.7 ± 0.4*	1.1 ± 0.1	2.5 ± 0.3*
9	Q99LC5	Electron transfer flavoprotein α	35009	8.62	6	95.5	5.4 ± 0.5*	1.1 ± 0.2	4.9 ± 0.4*
10	P56391	Cytochrome c oxidase subunit 6B1	10071	8.96	9	100	2.6 ± 0.6*	1.2 ± 0.2	2.2 ± 0.3*

Criteria for positive identifications from three independent experiments consisted of two peptides or more, a MS/MS confidence interval (C.I.) of 95% or higher, a correct molecular mass and pI position, and identification from all 2D gels. Proteins reported were all rank No.1 proteins and no other protein identification with high C.I.% was observed. –, detected in IPC hearts but undetectable in perfusion control and MβCD + IPC hearts. A ratio > 1.5 indicated significant differences between groups ($n = 3$, *, $p < 0.05$).

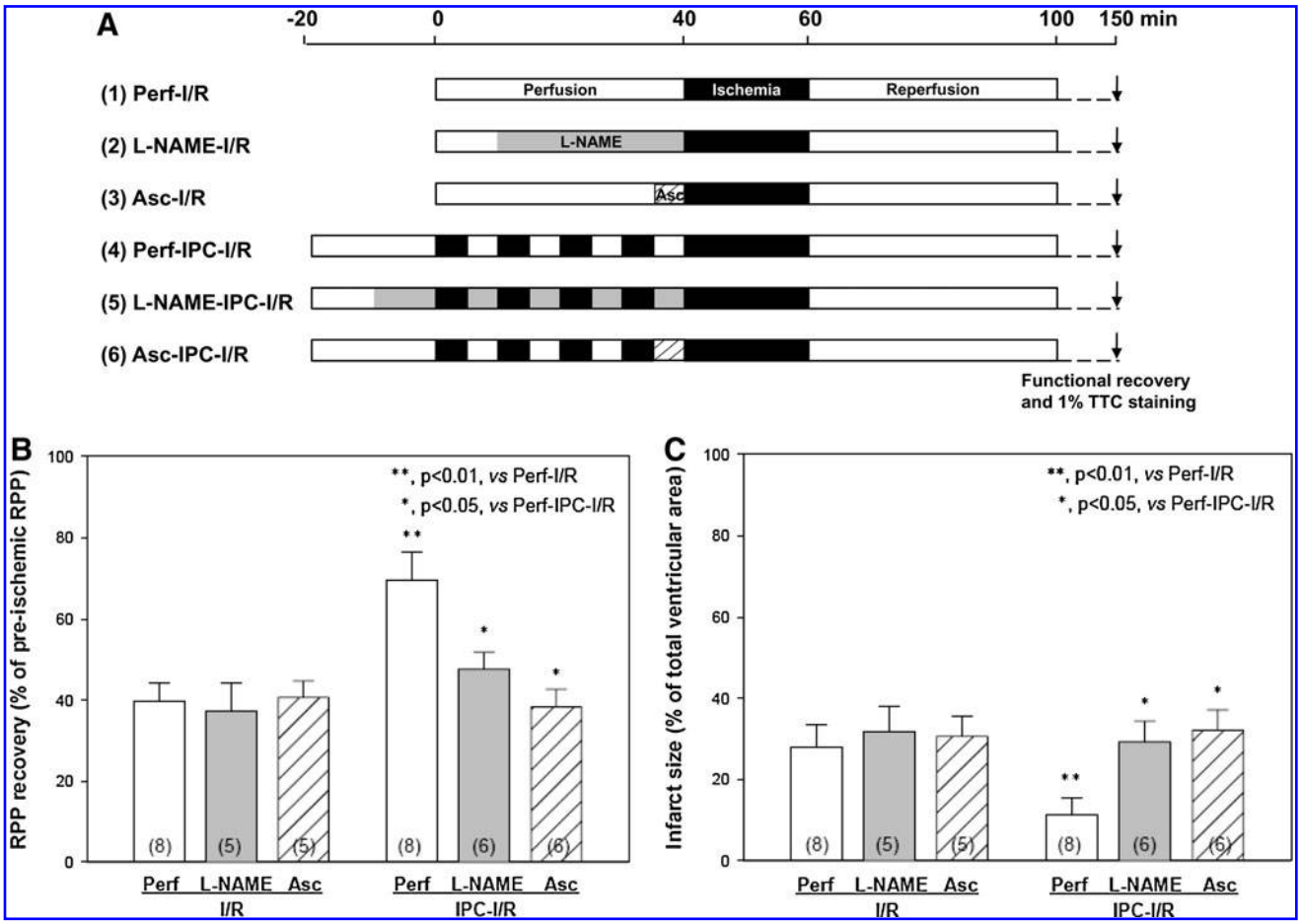

FIG. 5. Inhibition of NO/SNO signaling abolished IPC-induced cardioprotection. (A) IPC-I/R protocol with L-NAME (10 μmol/L) or ascorbic acid (1 mmol/L) administration; **(B)** Post-ischemic left ventricular RPP functional recovery; **(C)** Infarct size, measured at the end of reperfusion by 1% TTC staining. *$p < 0.05$ *vs*. Perf-IPC-I/R, and **$p < 0.01$ *vs*. Perf-I/R; *n*, number of animals in each group. Because ascorbic acid reduced LVDP by ~50%, we also provided LVDP values (cm H_2O) at the end of reperfusion for all the groups: Perf-IR (53 ± 9), Asc-I/R (56 ± 5); IPC-I/R (98 ± 8) and Asc-IPC-I/R (50 ± 6).

homogenizer. These total heart homogenates were snap frozen in liquid nitrogen and stored at −80°C.

Mitochondria isolation

Mitochondria were rapidly isolated by differential centrifugation according to standard procedures (40) immediately after perfusion or IPC protocol. Briefly, hearts were minced in mitochondria isolation buffer (pH 7.25, in mmol/L: 225 mannitol, 75 sucrose, 5 MOPS, 2 taurine, and 0.5 EGTA) and homogenized with a Polytron. Trypsin (0.001 g/0.1 g wet tissue) was added to the homogenate for 5 min on ice. Digestion was stopped by adding isolation buffer containing protein protease/phosphatase inhibitors. The homogenate was centrifuged at 500 *g* for 5 min, and the resulting supernatant was spun at 11,000 *g* for 5 min to pellet the mitochondria. The final mitochondrial pellet was resuspended in isolation buffer with protein protease/phosphatase inhibitors. Protein content was determined using a Bradford assay.

Detergent-free isolation of caveolae-enriched fractions

Caveolae-enriched fractions were isolated using a protocol modified from Song *et al.* (32) using a discontinuous (5%/35%/45%, w/v) sucrose gradient ultracentrifugation in buffer containing (pH 6.5, in mmol/L): 25 2-(N-morpholino)ethanesulfonic acid, 150 NaCl, and 1 EDTA. After ultracentrifugation at 200,000 *g* for 18 h at 4°C in a Beckman SW 41 swinging bucket rotor, the sucrose gradient was collected in 1 ml fractions from the top to the bottom. A light-scattering band confined to the 5%–35% sucrose interface was observed and collected as the caveolae-enriched fraction (fraction 5 as shown in Fig. 1B).

Transmission electron microscopy

Perfusion control ($n = 4$) and MβCD-infused ($n = 3$) hearts were examined for ultrastructural changes. Following treatment, hearts were perfused for 2 min with a relaxing buffer (pH 7.2, in mmol/L: 80 potassium acetate, 10 potassium phosphate, and 5 EGTA) followed with the fixative (5% glutaraldehyde in 0.12 mol/L of sodium cacodylate, pH 7.35). Hearts were dissected, samples of left ventricular myocardium were removed and put into fresh fixative for 1 h at 4°C. Samples were postfixed in 1% osmium tetroxide, en bloc stained with 1% uranyl acetate, dehydrated with an ethanol series and propylene oxide, then embedded in EMbed-812 (Electron Microscopy Sciences, Hatfield PA). Thin sections were stained with uranyl acetate and lead citrate.

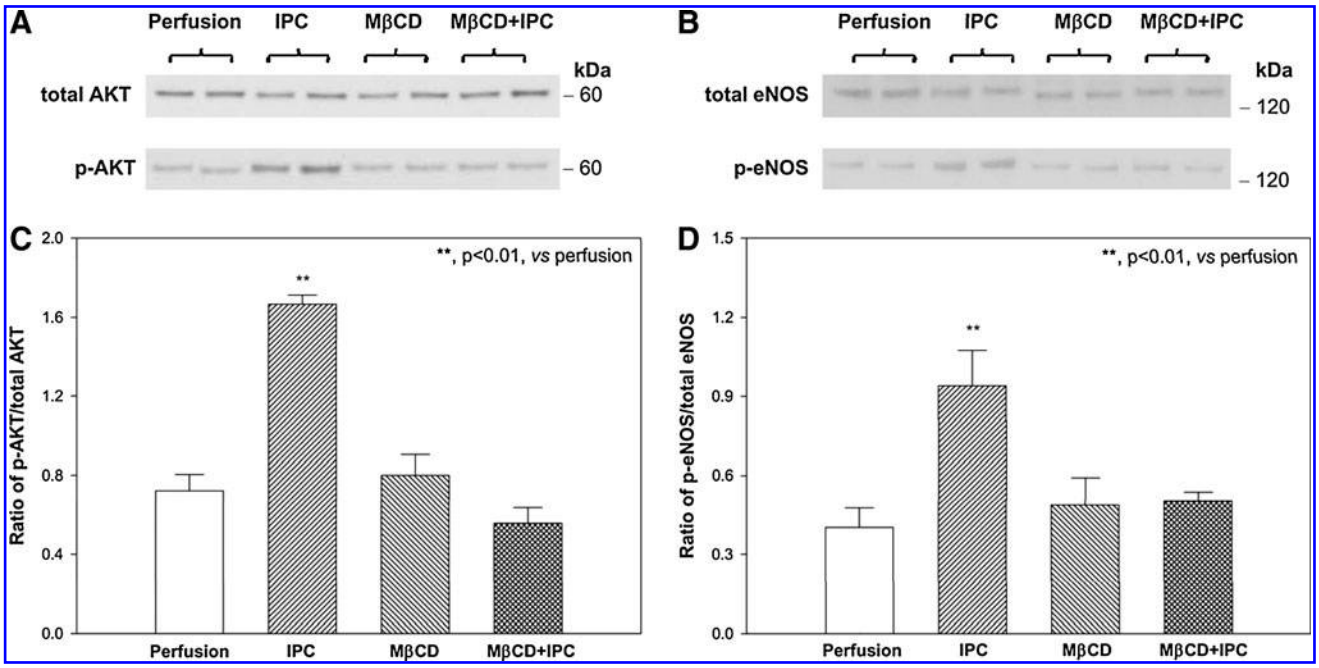

FIG. 6. MβCD treatment blocked IPC-induced phosphorylation and activation of AKT and eNOS. The total homogenates isolated from two mouse hearts for each group were subjected to 4%–12% SDS-PAGE, followed by anti-p(Ser473)-AKT/total AKT **(A)** and anti-p(Ser1177)-eNOS/total eNOS. **(B)** Immunoblot detection. *Top panels*: representative immunoblots. *Bottom panels*: densitometric analysis for the ratio of p-AKT/total AKT **(C)** and p-eNOS/total eNOS **(D).** $^{**}p < 0.01$, *vs.* perfusion control ($n = 4$ in each group).

Electron microscopy was performed on a JEM 1400 electron microscope (JEOL USA, Peabody MA) with an AMT XR-111 digital camera (Advanced Microscopy Techniques Corporation, Woburn MA). The number of caveolae/μm membrane length was counted on more than 40 cross-section images taken at 10,000X magnification for each sample.

Identification of SNO proteins by 2D DyLight DIGE

The modified biotin switch method (13) using DyLight-maleimide sulfhydryl-reactive fluors (Pierce Biotechnology, Rockford, IL) was applied to identify SNO proteins (19, 33). Since MβCD treatment caused disruption of caveolae, the

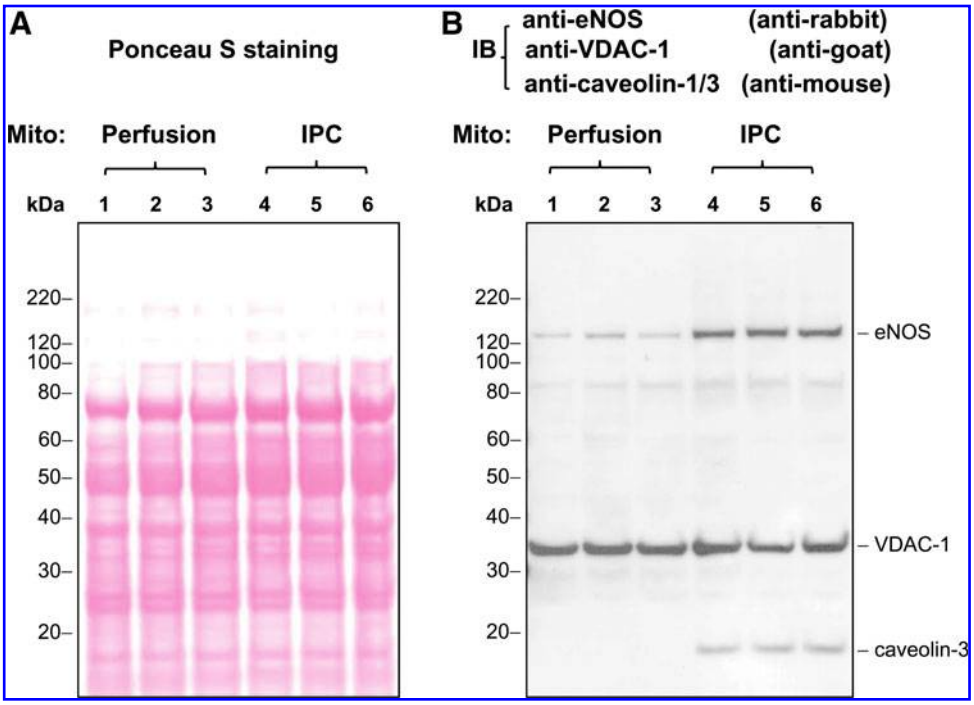

FIG. 7. IPC increases association of caveolin 3 and eNOS with mitochondria. Mitochondria isolated from three mouse hearts for each group were subjected to 4%–12% SDS-PAGE, followed with Ponceau S staining **(A)** and anti-eNOS, VDAC-1, caveolin-1, and caveolin-3 immunoblots **(B).** (To see this illustration in color the reader is referred to the web version of this article at www.liebertonline.com/ars).

total heart homogenates rather than caveolae-enriched fractions isolated from MβCD-treated mouse hearts were used for 2D DyLight DIGE study. After the DyLight switch and labeling, equal amounts (250 μg) of each sample were mixed together and subjected to 2D DyLight DIGE. Each gel was scanned at the unique excitation/emission wavelengths of each DyLight fluor using a Typhoon 9400 imager (GE Healthcare Life Sciences, Piscataway, NJ) at a resolution of 100 μm. Image analysis software PG240 v2006 (Nonlinear Dynamics, Newcastle upon Tyne, UK) was used to align, detect, match, and pick spots for each DyLight image. The method selected for spot normalization was total spot volume using the scaling factor total area where the volume of each spot is divided by the total volume of all of the spots in the image multiplied by a scaling factor. Protein spots were chosen for identification with mass spectrometry if they exhibited a >1.5-fold difference volume intensity between IPC and perfusion control with a value of $p < 0.05$. The Ettan Spot Handling Workstation (GE Healthcare Life Sciences) performed automated extraction of the selected protein spots followed by in-gel trypsin digestion. Protein identification was carried out using a MALDI-TOF/TOF instrument (4700 Proteomics Analyzer, Applied Biosystems, Carlsbad, CA) in positive ion mode with a reflector. For MS analysis, an 800–4000 m/z mass range was used with 1500 shots per spectrum. Result dependent analysis (RDA) was used for MS/MS selection. A maximum of six precursors per protein were selected with a confidence interval (C.I.) percentage of 50 or higher with a minimum signal/noise ratio of 50. In addition, a low confidence investigation (peptides not matched to top proteins) was used to allow a maximum of 5 precursors per spot with minimum signal/noise ratio of 50 selected for data-dependent MS/MS analysis. A 1-kV collision energy was used for collision-induced dissociation (CID), and 1500 acquisitions were accumulated for each MS/MS spectrum. For both MS and MS/MS analysis, the default calibration was calibrated with a 4700 mass standard peptide mix (Applied Biosystems) achieving a mass accuracy within 50 ppm. The peak-list generating software used was GPS Explorer software, set to default parameters (version 3.0, Applied Biosystems). Mascot search engine (version 2.2, Matrix Science, Boston, MA) was used for peptide and protein identifications. Swiss-Prot Protein knowledgebase database (Sprot 2010.01.19) was searched against and MS peak filtering was set for all trypsin autolysis peaks. The taxonomy selected was Mus musculus (mouse), 46,021 protein sequences. The acceptance criteria for individual MS/MS spectra had a significance threshold set to $p < 0.05$ with expectation values <0.05 (number of different peptides with scores equivalent to or better than the result reported that are expected to occur in the database search by chance). The p value was chosen to reflect a 95% probability that the protein identification is correct. The positive identifications criteria were two peptides or more, a MS/MS C.I. of 95% or higher, a correct molecular mass and pI position, and identification from all 2D gels.

Immunoprecipitation and Western blot analysis

Mouse monoclonal anti-caveolin-3 and/or anti-caveolin-1 antibody (BD Biosciences, San Jose, CA) was used in the immunoprecipitation (IP) study along with Dynabeads Protein G and DynaMag^{TM}-2 (Invitrogen, Carlsbad, CA) according to the product instruction. The Dynabeads (1.5 mg) were washed and resuspended in 200 μl of IP buffer (phosphate-buffered saline containing 0.05% Tween-20 and protein protease/phosphatase inhibitors). Five μg of negative control mouse IgG1, anti-caveolin-1, anti-caveolin-3, or both monoclonal antibodies were added and incubated at room temperature for 30 min with gentle agitation to form Dynabead-antibody complex. After washing, the total homogenate ($\sim$500 μg) of each heart sample was added and the mixture was incubated at room temperature for 30 min with gentle agitation. After five washes with 500 μl of IP buffer, the Dynabeads were resuspended into 80 μl of 1 $\times$ NuPAGE LDS sample buffer with 10% (v/v) 2-mercaptoethanol, and heated for 10 min at 70°C. The extract was subjected to SDS-PAGE.

Equal volumes (from caveolae fractions) or equal amounts of total heart homogenate protein were separated by 4%–12% Bis-Tris SDS-PAGE (Invitrogen) and transferred to a nitrocellulose membrane. After the transfer, the membrane was stained with Ponceau S and then washed with TBS-T composed of (pH 8.0, in mmol/L) 10 Tris, 150 NaCl, and 0.1% (v/v) Tween 20. TBS-T supplemented with 5% (w/v) nonfat dry milk was used for the blocking solution. The antibodies were diluted as follows: 1:5000 for mouse monoclonal anti-caveolin-3 antibody (#610421, BD Biosciences), 1:1000 for mouse monoclonal anti-caveolin-1 antibody (#610407, BD Biosciences), 1:200 for goat polyclonal anti-VDAC-1 (#sc-8828) and anti-eNOS (#sc-654, Santa Cruz), and 1:1000 for rabbit polyclonal antibodies including anti-phospho(Ser473)-AKT (#9271S), anti-AKT (#9272), and anti-phospho(Ser1177)-eNOS (#9570) antibodies (Cell Signaling, Danvers, MA). The corresponding IgG HRP-conjugated secondary antibodies (1:5000 dilution, Cell Signaling) were used in combination with a chemiluminescent substrate (GE Healthcare Life Sciences) according to standard procedures.

Data analysis

Results are expressed as mean $\pm$ SE. Statistical significance was determined by Student's t test or ANOVA as required. Differences were regarded to be significant at $^{*}p < 0.05$, and $^{**}p < 0.01$.

Acknowledgments

This work was supported by the NIH Intramural Program (JS, TN, AA, PC, SE, MG, MD and EM), NIH grants 1F32HL096142 (MK), and 5R01HL039752 (CS).

Author Disclosure Statement

No competing financial interests exist.

References

1. Barouch LA, Harrison RW, Skaf MW, Rosas GO, Cappola TP, Kobeissi ZA, Hobai IA, Lemmon CA, Burnett AL, O'Rourke B, Rodriguez ER, Huang PL, Lima JAC, Berkowitz DE, and Hare JM. Nitric oxide regulates the heart by spatial confinement of nitric oxide synthase isoforms. *Nature* 416: 337–339, 2002.
2. Chen W, Gabel S, Steenbergen C, and Murphy E. A redox-based mechanism for cardioprotection induced by ischemic preconditioning in perfused rat heart. *Circ Res* 77: 424–429, 1995.

3. Cohen MV, Yang X-M, and Downey JM. Nitric oxide is a preconditioning mimetic and cardioprotectant and is the basis of many available infarct-sparing strategies. *Cardiovasc Res* 70: 231–239, 2006.
4. Das M, Gherghiceanu M, Lekli I, Mukherjee S, Popescu LM, and Das DK. Essential role of lipid raft in ischemic preconditioning. *Cell Physiol Biochem* 21: 325–334, 2008.
5. Dessy C, Feron O, and Balligand J-L. The regulation of endothelial nitric oxide synthase by caveolin: a paradigm validated *in vivo* and shared by the 'endothelium-derived hyperpolarizing factor'. *Pflügers Arch* 459: 817–827, 2010.
6. Feron O and Balligand J-L. Caveolins and the regulation of endothelial nitric oxide synthase in the heart. *Cardiovasc Res* 69: 788–797, 2006.
7. Feron O, Belhassen L, Kobzik L, Smith TW, Kelly RA, and Michel TE. Endothelial nitric oxide synthase targeting to caveolae. Specific interactions with caveolin isoforms in cardiac myocytes and endothelial cells. *J Biol Chem* 271: 22810–22814, 1996.
8. Guo Y, Li Q, Wu W-J, Tan W, Zhu X, Mu J, and Bolli R. Endothelial nitric oxide synthase is not necessary for the early phase of ischemic preconditioning in the mouse. *J Mol Cell Cardiol* 44: 496–501, 2008.
9. Hausenloy D, Ong S-B, and Yellon D. The mitochondrial permeability transition pore as a target for preconditioning and postconditioning. *Basic Res Cardiol* 104: 189–202, 2009.
10. Horikawa YT, Patel HH, Tsutsumi YM, Jennings MM, Kidd MW, Hagiwara Y, Ishikawa Y, Insel PA, and Roth DM. Caveolin-3 expression and caveolae are required for isoflurane-induced cardiac protection from hypoxia and ischemia/reperfusion injury. *J Mol Cell Cardiol* 44: 123–130, 2008.
11. Insel PA, Head BP, Ostrom RS, Patel HH, Swaney JS, Tang CM, and Roth DM. Caveolae and lipid rafts: G protein-coupled receptor signaling microdomains in cardiac myocytes. *Ann NY Acad Sci* 1047: 166–172, 2005.
12. Iwakiri Y, Satoh A, Chatterjee S, Toomre DK, Chalouni CM, Fulton D, Groszmann RJ, Shah VH, and Sessa WC. Nitric oxide synthase generates nitric oxide locally to regulate compartmentalized protein S-nitrosylation and protein trafficking. *Proc Natl Acad Sci USA* 103: 19777–19782, 2006.
13. Jaffrey SR and Snyder SH. The biotin switch method for the detection of S-nitrosylated proteins. *Sci STKE* 86: PL1, 2001.
14. Jones SP and Bolli R. The ubiquitous role of nitric oxide in cardioprotection. *J Mol Cell Cardiol* 40: 16–23, 2006.
15. Kohr MJ, Sun J, Aponte A, Wang G, Gucek M, Murphy E, and Steenbergen C. Simultaneous measurement of protein oxidation and S-nitrosylation during preconditioning and ischemia/reperfusion injury with resin-assisted capture. *Circ Res* 108: 418–426, 2011.
16. Koneru S, Penumathsa SV, Thirunavukkarasu M, Samuel SM, Zhan L, Han Z, Maulik G, Das DK, and Maulik N. Redox regulation of ischemic preconditioning is mediated by the differential activation of caveolins and their association with eNOS and GLUT-4. *Am J Physiol* 292: H2060–H2072, 2007.
17. Lima B, Forrester MT, Hess DT, and Stamler JS. S-Nitrosylation in cardiovascular signaling. *Circ Res* 106: 633–646, 2010.
18. Lima B, Lam GKW, Xie L, Diesen DL, Villamizar N, Nienaber J, Messina E, Bowles D, Kontos CD, Hare JM, Stamler JS, and Rockman HA. Endogenous S-nitrosothiols protect against myocardial injury. *Proc Natl Acad Sci USA* 106: 6297–6302, 2009.
19. Lin J, Steenbergen C, Murphy E, and Sun J. Estrogen receptor-b activation results in S-nitrosylation of proteins involved in cardioprotection. *Circulation* 120: 245–254, 2009.
20. Maniatis NA, Brovkovych V, Allen SE, John TA, Shajahan AN, Tiruppathi C, Vogel SM, Skidgel RA, Malik AB, and Minshall RD. Novel mechanism of endothelial nitric oxide synthase activation mediated by caveolae internalization in endothelial cells. *Circ Res* 99: 870–877, 2006.
21. Michel T and Vanhoutte P. Cellular signaling and NO production. *Pflügers Arch* 459: 807–816, 2010.
22. Murphy E and Steenbergen C. Preconditioning: The mitochondrial connection. *Annu Rev Physiol* 69: 51–67, 2007.
23. Murry C, Jennings R, and Reimer K. Preconditioning with ischemia: A delay of lethal cell injury in ischemic myocardium. *Circulation* 74: 1124–1136, 1986.
24. Parton RG and Simons K. The multiple faces of caveolae. *Nat Rev Mol Cell Biol* 8: 185–194, 2007.
25. Patel HH, Head BP, Petersen HN, Niesman IR, Huang D, Gross GJ, Insel PA, and Roth DM. Protection of adult rat cardiac myocytes from ischemic cell death: Role of caveolar microdomains and delta-opioid receptors. *Am J Physiol* 291: H344–H350, 2006.
26. Patel HH, Murray F, and Insel PA. Caveolae as organizers of pharmacologically relevant signal transduction molecules. *Annu Rev Pharmacol Toxicol* 48: 359–391, 2008.
27. Quinlan CL, Costa ADT, Costa CL, Pierre SV, Dos Santos P, and Garlid KD. Conditioning the heart induces formation of signalosomes that interact with mitochondria to open mitoKATP channels. *Am J Physiol* 295: H953–H961, 2008.
28. Sanchez FA, Rana R, Kim DD, Iwahashi T, Zheng R, Lal BK, Gordon DM, Meininger CJ, and Duran WN. Internalization of eNOS and NO delivery to subcellular targets determine agonist-induced hyperpermeability. *Proc Natl Acad Sci USA* 106: 6849–6853, 2009.
29. Schulman IH and Hare JM. Regulation of cardiovascular cellular processes by S-nitrosylation. *Biochim Biophys Acta* In press, 2011.
30. Shaul PW. Regulation of endothelial nitric oxide synthase: Location, location, location. *Annu Rev Physiol* 64: 749–774, 2002.
31. Simoncini T, Hafezi-Moghadam A, Brazil DP, Ley K, Chin WW, and Liao JK. Interaction of oestrogen receptor with the regulatory subunit of phosphatidylinositol-3-OH kinase. *Nature* 407: 538–541, 2000.
32. Song KS, Scherer PE, Tang Z, Okamoto T, Li S, Chafel M, Chu C, Kohtz DS, and Lisanti MP. Expression of caveolin-3 in skeletal, cardiac, and smooth muscle cells. Caveolin-3 is a component of the sarcolemma and co-fractionates with dystrophin and dystrophin-associated glycoproteins. *J Biol Chem* 271: 15160–15165, 1996.
33. Sun J, Morgan M, Shen R-F, Steenbergen C, and Murphy E. Preconditioning results in S-nitrosylation of proteins involved in regulation of mitochondrial energetics and calcium transport. *Circ Res* 101: 1155–1163, 2007.
34. Sun J and Murphy E. Protein S-nitrosylation and cardioprotection. *Circ Res* 106: 285–296, 2010.
35. Talukder MAH, Yang F, Shimokawa H, and Zweier JL. eNOS is required for acute *in vivo* ischemic preconditioning of the heart: Effects of ischemic duration and sex. *Am J Physiol* 299: H437–H445, 2010.

36. Tang Z, Scherer PE, Okamoto T, Song K, Chu C, Kohtz DS, Nishimoto I, Lodish HF, and Lisanti MP. Molecular cloning of caveolin-3, a novel member of the caveolin gene family expressed predominantly in muscle. *J Biol Chem* 271: 2255–2261, 1996.
37. Tong H, Rockman HA, Koch WJ, Steenbergen C, and Murphy E. G protein-coupled receptor internalization signaling is required for cardioprotection in ischemic preconditioning. *Circ Res* 94: 1133–1141, 2004.
38. Tsutsumi YM, Horikawa YT, Jennings MM, Kidd MW, Niesman IR, Yokoyama U, Head BP, Hagiwara Y, Ishikawa Y, Miyanohara A, Patel PM, Insel PA, Patel HH, and Roth DM. Cardiac-specific overexpression of caveolin-3 induces endogenous cardiac protection by mimicking ischemic preconditioning. *Circulation* 118: 1979–1988, 2008.
39. Wang Y, Ahmad N, Kudo M, and Ashraf M. Contribution of Akt and endothelial nitric oxide synthase to diazoxide-induced late preconditioning. *Am J Physiol* 287: H1125–H1131, 2004.
40. Wong R, Aponte AM, Steenbergen C, and Murphy E. Cardioprotection leads to novel changes in the mitochondrial proteome. *Am J Physiol* 298: H75–H91, 2010.
41. Xu KY, Huso DL, Dawson TM, Bredt DS, and Becker LC. Nitric oxide synthase in cardiac sarcoplasmic reticulum. *Proc Natl Acad Sci USA* 96: 657–662, 1999.

Address correspondence to:
Dr. Junhui Sun
Systems Biology Center
National Heart Lung and Blood Institute
National Institutes of Health
10 Center Drive, Bldg10/Rm8N206
Bethesda, MD 20892

E-mail: sun1@mail.nih.gov

Date of first submission to ARS Central, December 15, 2010; date of final revised submission, July 7, 2011; date of acceptance, July 10, 2011.

Abbreviations Used

2D DIGE = two-dimensional differences in gel electrophoresis
AKT = protein kinase B
eNOS = endothelial nitric oxide synthase
IPC = ischemic preconditioning
I/R = ischemia/reperfusion
MβCD = methyl-β-cyclodextrin
NO = nitric oxide
SNO = S-nitrosylation

This article has been cited by:

1. Junhui Sun, Angel M. Aponte, Mark J. Kohr, Guang Tong, Charles Steenbergen, Elizabeth Murphy. 2012. Essential role of nitric oxide in acute ischemic preconditioning: S-Nitros(yl)ation versus sGC/cGMP/PKG signaling?. *Free Radical Biology and Medicine* . [CrossRef]